Journal of the Earth & Space Physics. Vol. 33, No. 3, 2008 13-24

3-Dimensional upper mantle velocity structure for Iranian Plateau revealed by P_n and S_n tomography

Tabatabai Mir, Sh[1]., Bergman, E[2]. and Gheitanchi, M. R[3*].

[1]*Ph.D. student of Geophysics, Institute of Geophysics, University of Tehran, Iran*
[2]*University of Colorado at Boulder, Department of Physics, USA*
[3]*Professor, Earth Physics Department, Institute of Geophysics, University of Tehran, Iran*

(Received: 13 Jan 2007 , Accepted: 8 Sep 2007)

Abstract

Studying crustal and upper mantel structures has been limited in the Iranian Plateau and there has been little work done in this field. In this paper we have a primary motive to map P_n and S_n velocities beneath most of the Iranian Plateau in order to test 3-D mantle models and to develop and test a method to produce P_n and S_n travel time correction surfaces that are the 3-D analogue of travel time curves for a 1-D model. To the new data set that we have relocated using HDC method which we have published in another paper; we apply the tomographic method of Barmin et al., augmented to include station and event corrections and an epicentral distance correction. The P_n and S_n maps are estimated on a 2^o x 2^o grid thoughout the Iranian Plateau. We define the phases P_n and S_n as arriving between epicentral distances of 3^o and 15^o. After selection, the resulting data set consists of 42,368 P_n and 10,897 S_n travel times distributed in-homogeneously across the Iranian Plateau. We used CRUST 5.1 as the starting Model. The P_n and S_n maps compare favorably with recent 3-D models of P and S in the uppermost mantle. The RMS misfit to the entire Iranian data set from the P_n and S_n model increases nearly linearly with distance and averages about 1.5 s for Pn and 3.1 s for S_n. Comparing with the starting model we have a better detail map of the region. Getting the vertical velocity derivative right may be more important in predicting regional travel times than mapping lateral variations. Recent models are providing new information about the vertical velocity gradient in the uppermost mantle which controls the depth of penetration. Further research remains to determine if these results improve regional location capabilities.

Key words: Iranian Plateau, Crustal velocity model, Upper mantle, Tomography, P_n and S_n velocities

1 INTRODUCTION

Determination of accurate seismic locations and uncertainties is of prime importance in studying geological features or seismotectonic evaluation of a region. In order to have a well constrained data set we need a better model of the crust and upper mantle. Sparse network locations are subject to significant bias due to regional variations in the structure of the crust and upper mantle.

This paper has a primary motive to map Pn and Sn velocities beneath most of the the Iranian Plateau using regional phase data (P_n, S_n) in order to test global (e.g., Ekstrom and Dziewonski, 1998; Bijwaard et al., 2000; Shapiro et al., 2000) and regional (e.g., Villasenor et al., 2001) 3-D seismic models and to develop and test a method to produce P_n and S_n Iranian travel time correction surfaces. These surfaces form a common basis for locating seismic events with regional data alone. Each travel time correction surface is a map centered on a specific seismic station. The value at each point on the map is the travel time observed at the station from a seismic event located at a specified depth. Usually the predicted travel times are presented relative to the prediction from a 1-D seismic model.

We have tried to use all the data we can to have dense ray path intersections The method to estimate P_n and S_n that we describe here is based heavily on earlier efforts by other researchers (e.g., Hearn et al., 1991). Our method and earlier incarnations suffer from a number of problems. These include the fact that P_n and S_n are not monolithic phases that turn at a uniform depth independent of epicentral distance and tectonic regime, and it is difficult to separate crustal from mantle contributions in the observed travel times. These problems are manifested more strongly on the P_n and S_n maps than on the predicted travel time correction surfaces. Thus, although the methods we employ may not provide ideal means to estimate mantle structures, they suffer far fewer problems in predicting the travel time corrections needed to improve capabilities to locate regional events. The results presented here should, therefore, be seen as a preliminary step toward

[*]Corresponding author: Tel: 021-61118235 Fax: 021-88630548 E-mail: mrghchee@ut.ac.ir

developing a unified model of the crust and uppermost mantle that result from simultaneous inversion of surface wave dispersion and regional body wave travel times.

In the following, we first discuss the data set and display the resulting travel time correction surfaces for stations and events. Second we discuss the tomographic method, and third we discuss the fit to the regional phase data and inferred uncertainties in the correction surfaces.

2 DATA

P_n and S_n travel times are taken from the catalogue of relocated earthquakes using the HDC method (Tabatabai Mir, 2007). ISC travel times are for events that occurred from 1964 through 1997 and NEIC data are from 1998 and 2004. We define the phases P_n and S_n as arriving between epicentral distances of 3o and 15o. P_n and S_n may dip into the mantle substantially, particularly beyond epicentral distances of~8o. The depth of penetration will depend on the vertical derivative of velocity, which will vary spatially. The truncation of the data set to include rays only if epicentral distances are less than 10^o-12^o, as in some other studies (e.g., Hearn and James, 1994), would severely restrict path coverage in some areas of the Iranian Plateau. To utilize longer paths it is desirable to correct for the effect of ray penetration into the uppermost mantle. This data set consists of 123, 290 P_n phases and 34, 870 S_n phases for 7980 events for P_n and 6255 events for S_n. Data are used in the inversion if the residual relative to the prediction from the 1-D model ak135 (Kennett et al., 1995) is less than 7.5 s for P and 15 s for S, if the event depth is within the crust or less than 50 km deep, if the azimuthal gap to all reporting stations for the event is less than 180 degrees, and if the nominal error ellipse is less than 1000 km2 in area. These selection criteria reduce the data set to 42368 Pn and 10897 Sn phases. Data density is shown in figure 1 and the ray traces are shown in figure 2.

Because path lengths for these phases are by definition short (<15o), paths only exist in regions where both sources and receivers are common. Thus, the path distribution is highly heterogeneous across the region.

We further reduce this data set by rejecting late arriving travel times at epicentral distances from 3^o to 6^o that may be misidentified crustal phases (e.g., Pg) or Moho reflections (PmP, SmS). In addition, in the tomography we reject measurements misfit by the starting model at more than 2σ, where σ is the average misfit produced by the starting model. This is done to help stabilize the station and event corrections. However, we report misfit statistics relative to the entire data set across the Iranian Plateau.

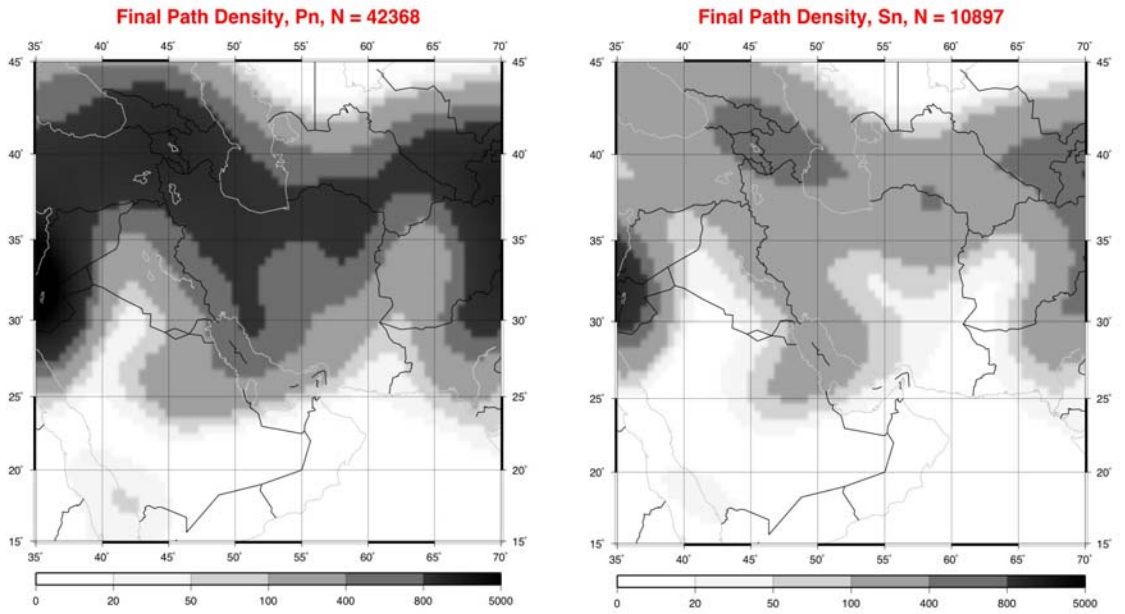

Figure 1. Path Density for P_n and S_n data, defined as the number of paths intersecting a 2^o x 2^o cell.

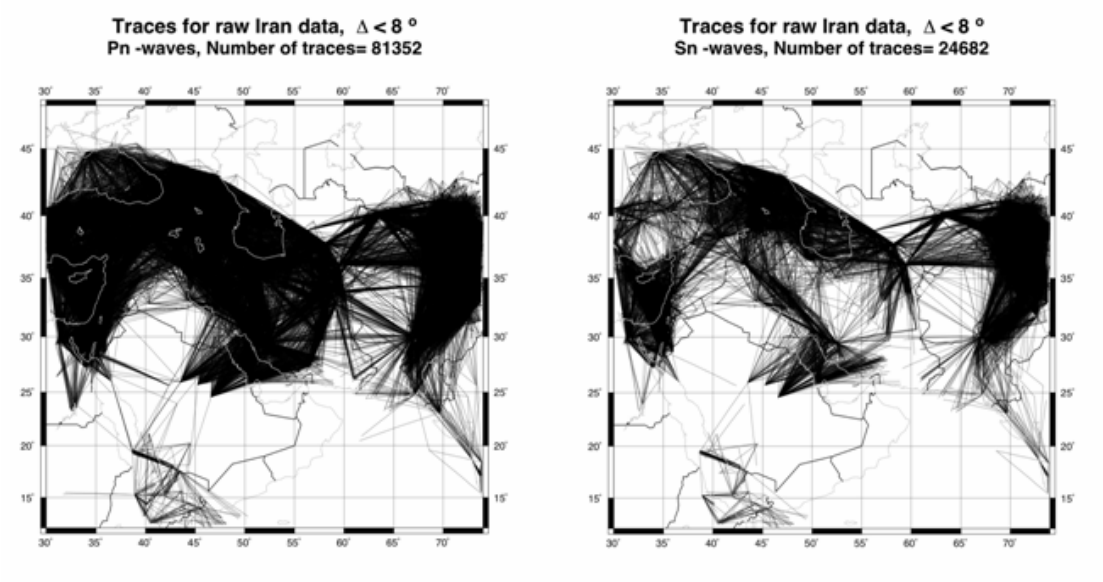

Figure 2. Ray Traces for P_n and S_n data.

3 METHOD

The observed travel time, t_{obs}, is modeled as follows:

$$t_{obs} = t_m + t_{crust-sta} + t_{crust-evt} + \delta t_{sta} + \delta t_{evt} + \delta t(\Delta) + \delta t_m \quad (1)$$

where t_m is the predicted travel time for rays through the mantle part of the input reference model, the contributions to the travel time due to the crustal part of the reference model on the event and station sides are $t_{cruststa}$ and t_{crust_evt}, the station and event delays or static corrections are δt_{sta} and δt_{evt}, $\delta t(\Delta)$ is the distance correction, δt_m is the travel time correction for the mantle part of the path, and Δ is epicentral distance. Thus, tm, t_{crust_sta}, and t_{crust_evt} are predicted by the reference model and δt_{sta}, δt_{evt}, $\delta t(\Delta)$, and δtm are estimated. If δvm is the velocity along path p in the reference model and δv_m is the model perturbation along the same path, then

$$t_m = \int_p \frac{ds}{vm} \quad (2)$$

$$\delta t_m = -\int_p \frac{\delta v_m}{v_m^2} ds \quad (3)$$

We assume that the ray through the perturbed model, $v_m + \delta_{vm}$, takes the same path as the ray through the reference model. In practice, we estimate the 2-D quantity δv_m from which we compute δtm for each ray p.

We use CRUST5.1 (Mooney et al., 1998) as the starting (reference) model in the crust and for mantle P and S. At each geographical point, CRUST5.1 only has one value of P and one value of S for the mantle, intended to characterize the velocity immediately below Moho. Thus, for the reference model the mantle leg of each path p is horizontal, following directly below Moho as shown in figure 3.

This is, in fact, a common approximation in P_n and S_n tomography, but realistic rays dive into the mantle to depths that depend on a non-zero vertical velocity derivative as figure 4b shows. Figure 4c attempts to quantify the error made by the horizontal ray approximation, by comparing the travel times diving into the mantle through a recent Eurasian 3-D model (Shapiro et al., 2000) with those computed for a model in which the rays propagate horizontally directly beneath Moho. The horizontal ray approximation produces an error that is a relatively smooth function of distance. For most of the continent, the estimated errors are similar and grade smoothly to a travel time error predicted to be about -2.4 s at 15o for P velocities. This motivates the introduction into equation (1) of a term that is a smooth function of distance, which we call the distance correction, $\delta t(\Delta)$. The correction $\delta t(\Delta)$ attempts to reduce the mantle velocities distributed in 3-D to a single 2-D datum surface which, by design, lies directly below Moho.

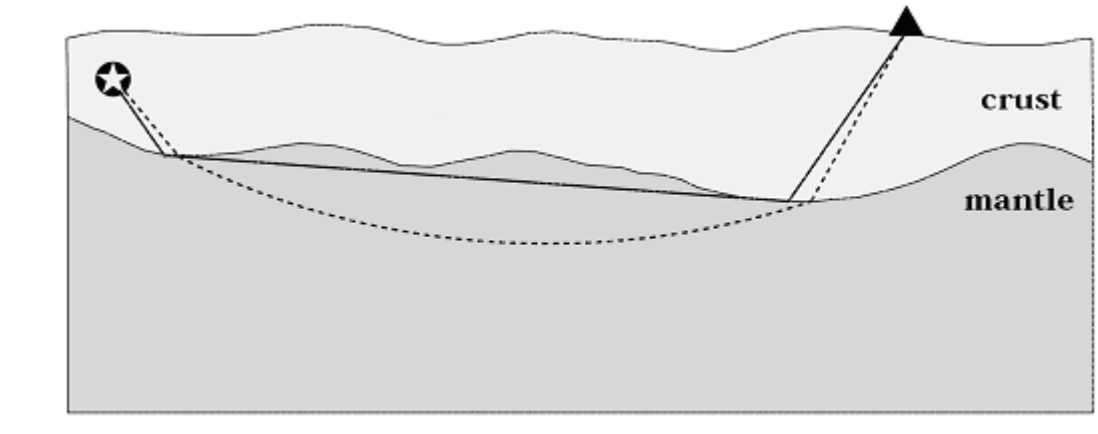

Figure 3. Illustration of sources of error in the tomography. Real ray paths(dashed line) follow different paths through both the crust and mantle than the hypothesized rays (solid lines) used in tomography. In particular, real paths dip deeper into the mantle as epicentral increases in a way that depends on the vertical velocity gradients.

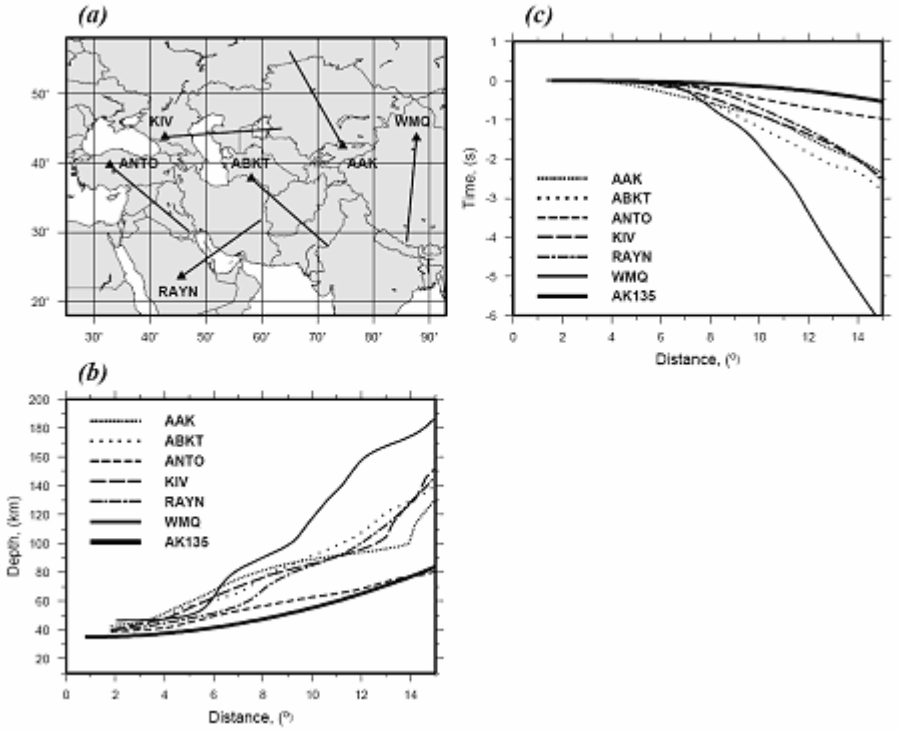

Figure 4. Examples to justify the distance correction, δt(Δ). (a) The location of the six 2-D velocity profiles used in (b) and (c). Each profile starts from a seismic station and runs for 15 degrees. The 3-D model used is that of Shapiro et al. (2000). (b) Turning point curves for the six profiles in (a) and for the 1-D model ak135. (c) Each curve is the difference between the travel time computed through the 3-D model of Shapiro et al. (2000) using the ray shooting method of Cerveny and Psencik (1988) and the travel time through the same model with a horizontal ray. This provides an estimate of the error in P- wave travel time caused by the horizontal ray approximation for the six profiles in (a).

Although the distance correction is an average across the continent, it allows us to fit data over a broader distance range than would be possible without the correction. We find that with this correction the tomographic maps agree well with those produced with short path data alone (epicentral distances less than 10^o) in those regions where tomographic maps can be constructed reliably using only the short path data. The use of a 3-D model to compute the distance correction is beyond the scope of the present work, but is an important direction for future research. We follow Hearn and collaborators (e.g., Hearn and Clayton, (1986); Hearn et al., (1991); Hearn and James, (1994); and elsewhere) and estimate event and station corrections. These corrections are designed to compensate for errors in the reference crustal model, errors in the prediction of the location of the mantle piercing points, and errors in event locations and origin times. A correction is estimated for a station if there are phase picks from at least seven events made at that station and an event correction is estimated for all events for which there are at least 10 reporting stations. The asymmetry in this condition is because there are more physical phenomena modeled with the event correction than with the station correction (e.g., mislocation, origin time error). The station and event corrections are undamped.

As presented here, the P_n and S_n maps are defined over a two-dimensional surface and, therefore, may be estimated with the same 2-D tomographic method we developed for surface wave tomography (Barmin et al., 2001). The inversion for Pn and Sn is approximately the same except that from the reference model we compute source and receiver side Moho penetration points and use these points as the starting and ending points of the ray during inversion. (See figure 3).

The approximation comes from the assumption that P_n and S_n rays are "horizontal" in a spherical mantle and propagate directly below Moho, as discussed above and depicted in figure 3.

In the method of Barmin et al. (2001), the model is constructed on an equally spaced grid such that the following figure-of-merit is minimized:

$$(\mathrm{Gm}-\mathrm{d})^{\mathrm{T}}\mathrm{C}^{-1}(\mathrm{Gm}-\mathrm{d})+\sum_{k=0}^{n}\alpha_k^2\left\|\mathrm{F}_k(\mathrm{m})\right\|^2+\sum_{k=0}^{n}\beta_k^2\left\|\mathrm{H}_k(\mathrm{m})\right\|^2, \quad (4)$$

which is a linear combination of data misfit, model roughness, and the amplitude of the perturbation to a reference model. The vector m represents the estimated model, δv_m, which is a perturbation relative to a reference across the region of interest, G is the forward operator that computes travel time from the estimated model, d is the data vector, C is the data covariance matrix or matrix of data weights, F is a Gaussian smoothing operator, and H is an operator that penalizes the norm of the model m in regions of poor data coverage. The spatial smoothing operator is defined over the 2-D model as follows;

$$\mathrm{F}_k(\mathrm{m})=\mathrm{m}_k(\mathrm{r})-\int_s \mathrm{S}_k(\mathrm{r},\mathrm{r}')\mathrm{m}_k(\mathrm{r}')\mathrm{d}\mathrm{r}', \quad (5)$$

where S_k is a smoothing kernel:

$$\mathrm{S}_k(\mathrm{r},\mathrm{r}')=\mathrm{K}_{ok}\exp\left(-\frac{|\mathrm{r}-\mathrm{r}'|^2}{2\sigma_k^2}\right) \quad (6)$$

$$\int_s \mathrm{S}_k(\mathrm{r},\mathrm{r}')\mathrm{d}\mathrm{r}'=1, \quad (7)$$

and σ_k is the spatial smoothing width or correlation length. The minimization of the expression in equation (5) explicitly ensures that the estimated model approximates a smoothed version of the model. The maps are estimated on a 2^o x 2^o grid across the Iranian Plateau with σ_k=150 km.

We refer to the Pn and Sn maps together with the parametric corrections δt_{sta}, δt_{evt}, and $\delta t(\Delta)$ as the CU P_n/S_n model to distinguish it from the recent 3-D models (e.g., Villasenor et al., 2001; Shapiro et al., 2000). To compute travel time correction surfaces, the distance correction, the station delays, and the P_n or S_n map must be used.

The method of Barmin et al. (2001) allows us to estimate 2ψ and 4ψ azimuthal anisotropy simultaneously with isotropic Pn and Sn. We find, however, that the estimates of azimuthal anisotropy are not robust with respect to data subsetting and variations in damping. In addition, the joint inversion for isotropic and anisotropic structures dominantly affects only the amplitudes of the isotropic maps, but no more so than the choice of isotropic damping which is largely arbitrary. Consequently, we report only isotropic P_n and S_n maps here and can safely ignore the effects of azimuthal anisotropy on these estimates.

4 TRAVEL TIME CORRECTION SURFACES

Travel time correction surfaces are a

computational convenience commonly used for locating seismic events with regional data alone. Each correction surface is a map centered on a specific seismic station. The value at each point on the map is the travel time predicted at the station from a seismic event at a specified depth. They are, therefore, the analogue for a 3-D model of travel time curves for 1-D models. Usually the predicted travel times are presented relative to the prediction from a 1-D seismic model. The accuracy of regional event locations will depend directly on the accuracy of the correction surfaces.

Using equations (1)-(3) and the notation defined in section 3, we define the travel time correction surface as follows:

$$t_{TTCS}(\Delta,\phi) = t_m(\Delta,\phi) + t_{crust-sta}(\Delta,\phi) + t_{crust-evt}(\Delta,\phi) + \delta t_{sta} + \delta t_{eut} + \delta t(\Delta) + \delta t_m(\Delta,\phi) - t_{1D}(\Delta), \quad (8)$$

where Δ and φ are distance and azimuth from the station to the event, respectively. The prediction from a 1-D model, t_{1D}, is subtracted so that the correction surface provides a residual relative to this reference.

Figure 5 displays P_n and S_n stations and events corrections. These surfaces are for P_n with surface sources and the station set at the local elevation. This differs from correction surfaces as they are commonly displayed in which both the source and station are on the reference ellipsoid. The anomaly is about 5 s and is typically twice this value for the Sn correction surface. Extending correction surfaces beyond 15^o will require using a 3-D model to compute the distance correction or the use of 3-D tomography.

5. P_n AND S_n TOMOGRAPHY

We estimate station delays δt_{sta}, event delays δt_{evt}, the distance correction curve $\delta t(\Delta)$, and the 2-D tomographic quantity $\delta v_m(\theta,\varphi)$ which represents lateral variations in seismic velocities in the uppermost mantle. Latitude and longitude are θ and φ, respectively. There are strong and essentially, unresolvable trade-offs between subsets of these quantities. For example, a constant velocity shift in the uppermost mantle could be fit either by a constant shift in δv_m or by introducing a linear trend in $\delta t(\Delta)$. The station delays, δt_{sta}, also strongly trade-off with δv_m directly beneath the station and the value of the distance correction at an epicentral distance of 3^o. The estimated values depend strongly on the inversion algorithm and the order in which the corrections are estimated, if the process is iterative rather than simultaneous. If the process were simultaneous then values would depend on the relative weights assigned to each correction. We constrain $\delta t(\Delta)$ to be approximately zero at 3o and let the curve $\delta t(\Delta)$ have only a moderate negative slope. Thus, we choose to fit much of the signal with station delays and allow a substantial constant shift in δv_m. Not surprisingly, the S_n corrections are typically larger than those for P_n, presumably because S variations in the crust and upper mantle are typically larger than P by about a factor of two. The P_n and S_n station delays are geographically coherent and correlate with one another with a poorly determined S/P ratio of about 1.8 relative to the mean of each distribution. Stations and events are not uniformly distributed over the continent, with stations predominantly in stable continental regions and events in tectonically deformed regions. For this reason, together with the fact that the delays are taken relative to a model, the delays are not expected to be zero-mean and in fact, display a positive mean for the stations and a negative mean for the events.

Although we estimate P_n corrections only for about 55% of the stations and half of the events and for S_n the numbers are about 45% and 20%, respectively, the great majority of the measurements emanate from events and are recorded at stations that have corrections. This is particularly true for P_n, where only about 3.5% of the measurements are made at stations without corrections and 13% are for events without event corrections. For S_n, the numbers are 4.5% and 35%, respectively. Thus, most measurements have the full complement of corrections applied. For stations and events for which we have not estimated corrections, we set the corrections equal to the mean of the distributions. The distance correction is shown in figure 6.

The shape of the P distance correction is different from that predicted, but the value of the correction at 15 degrees is about the same (~-2.5 s). There is in addition, a constant offset in δv_m equal to about -100 m/s relative to the average S_n velocity of CRUST5.1. We have greater confidence in the decisions we reached to resolve the trade-off between δvm and $\delta t(\Delta)$ for P than for S. The estimated P_n and S_n maps are shown in figure 7 and 8. Because our tomographic method penalizes the amplitude of the maps in regions of poor data coverage and the estimated maps are perturbations to a reference state, the maps revert

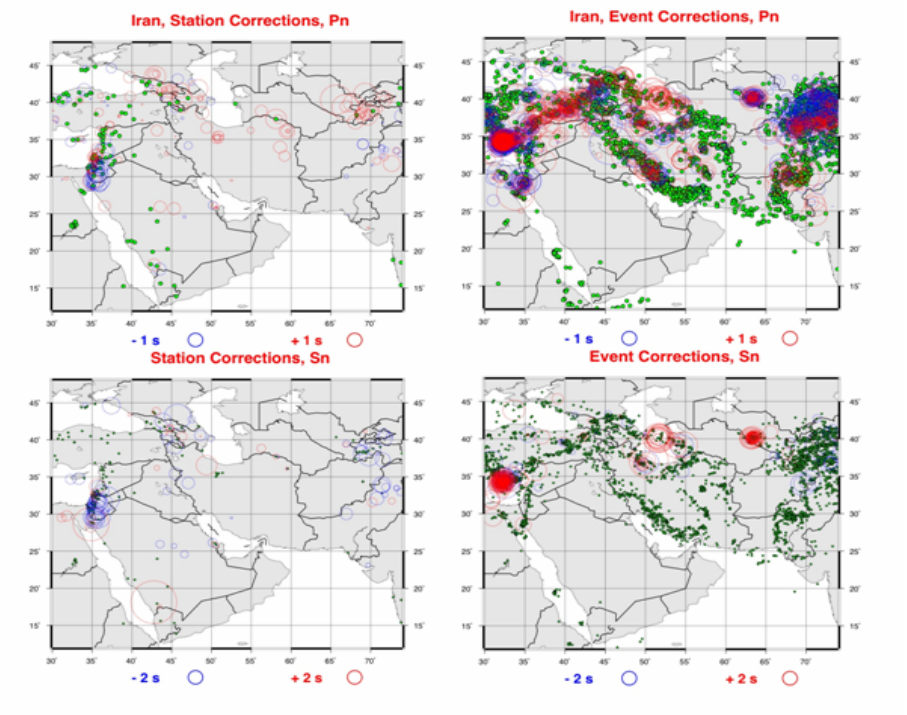

Figure 5. P_n and S_n stations and events corrections.

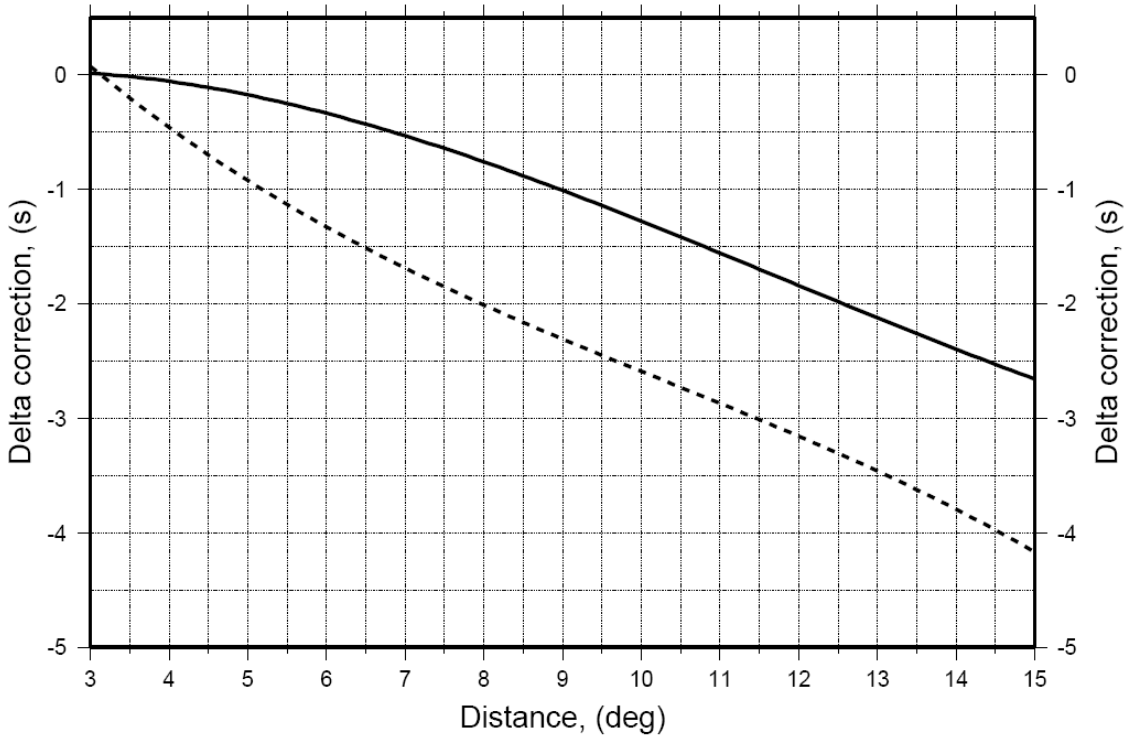

Figure 6. Estimated distance correction, $\delta t(\Delta)$, for P_n (solid line) and S_n (dashed line). The distance corrections are constrained to be approximately zero at an epicentral distance of 3^o.

to the reference model where data coverage is poor; i.e. less than 15 - 20 paths for each 2^o x 2^o cell. The areas of poor data coverage are identified as white regions in figure 6 and 7. The P_n and S_n anomalies in figure 7 and 8 are highly correlated and differ in amplitude by about a factor of two, such that $\delta v_s/v_s \sim 2\delta v_p/v_p$. The anomalies also compare well with known tectonic features and with the patterns of velocity variations at the top of the upper mantle in the 2^o x 2^o 3-D shear velocity model of Villasenor et al. (2001).

Smaller scale features however, are apparent in the P_n and S_n maps presented here and the amplitudes of the Sn map are somewhat larger than in the 3-D S model. Villasenor et al. (2001) also show that the anomalies are similar to those inthe teleseismic P model of Bijwaard et al. (1998) and Engdahl and Ritzwoller (2001) demonstrate that the anomalies correlate with teleseismic station corrections. Thus, the patterns of high and low velocities are robust and are apparent in a number of different data sets at both regional and global scales.

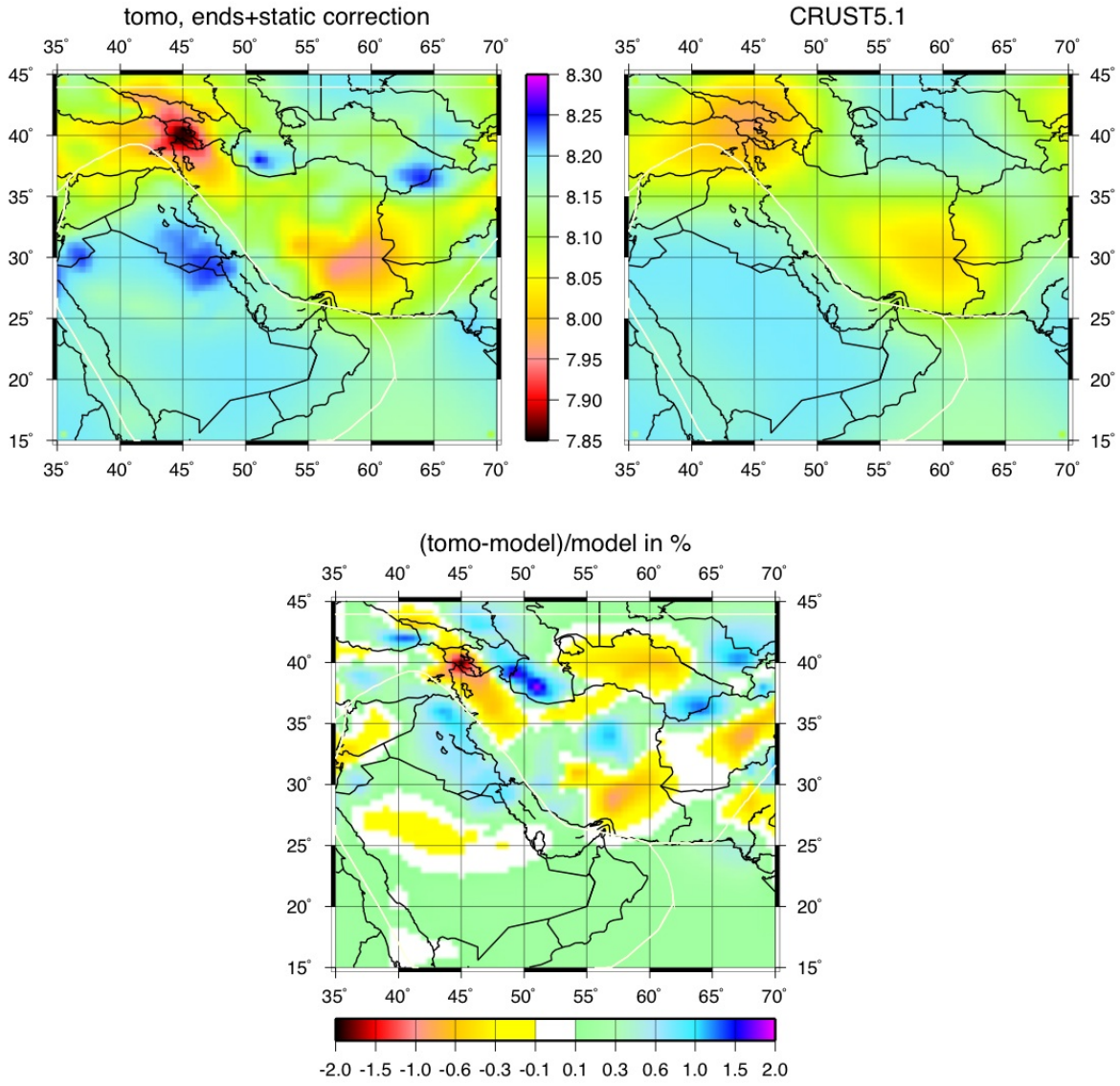

Figure 7. P_n Map estimated across the Iranian Plateau. Values are relative to the prediction from ak135 at the top of the mantle, 8.04 km/s for P_n.

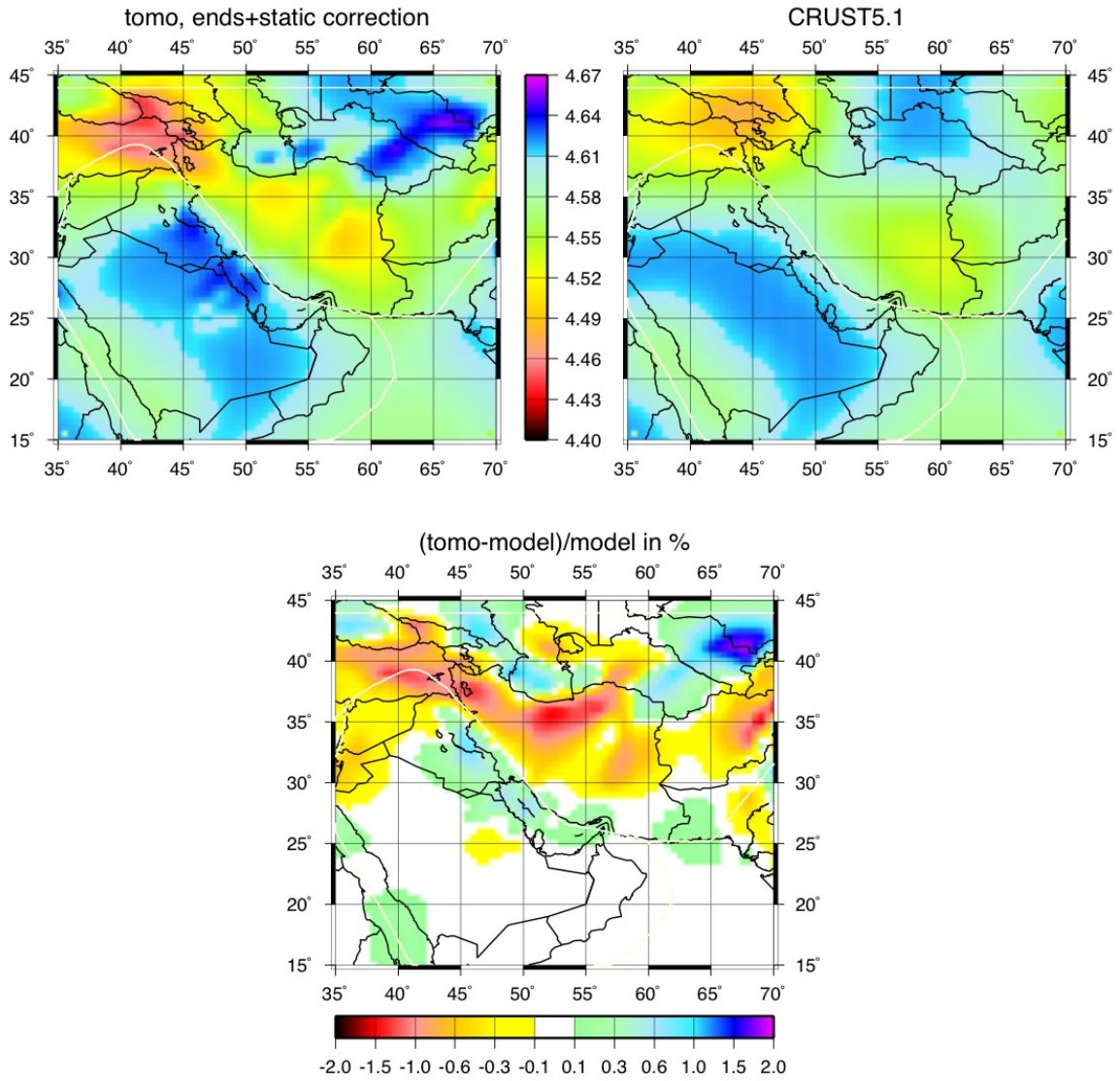

Figure 8. S_n Map estimated across the Iranian Plateau. Values are relative to the prediction from ak135 at the top of the mantle, 4.48 km/s for S_n.

6 DISCUSSION AND CONCLUSION

Misfits to the entire Iranian Plateau data set and overall summary statistics for P_n and S_n are presented in table 1.

The standard deviation σ reported in table 1 is computed relative to the distance-dependent mean, so that it represents the scatter around a trend. In general, short distance vertical offsets result in part from errors in the crustal model, either in average crustal velocities or Moho depths. Errors in the uppermost mantle velocities and vertical velocity gradients manifest themselves as trends with distance. The 1-D model ak135 does very well for P. Improvements afforded by the CU P_n/S_n model over ak135 are largest at epicentral distances greater than about 8o. S misfits from ak135, however, exhibit a strong distance trend, presumably because it is vertically nearly constant from Moho to about 200 km. Thus, the misfit trend in S for ak135 probably results from an error in the vertical gradient in the uppermost mantle. For both P and S, CRUST5.1 is too slow in the crust and S is on average too fast in the uppermost mantle. The overall rms misfit for the CU P_n/S_n is 1.5 s across all of

Eurasia for P_n and approximately twice this value for S_n. The entire Iranian Plateau data set is very noisy and many locations and origin times are poorly known. The residuals based on distance for these three models are summarized in figure 9.

The main purpose of this paper is to assess P_n and S_n tomography as a potential means of improving location capabilities using regional phase data alone. A full discussion of the velocity anomalies that appear in the P_n and S_n maps, therefore, is well beyond the intended scope of this paper. For greater coherence, however, we mention some of the characteristics of the estimated maps that agree with shear velocity anomalies that have emerged from surface wave dispersion studies (e.g., Shapiro et al., 2000; Villasenor et al., 2001). It should be remembered that Pn and Sn maps are of velocities right at the top of the mantle and are mute about vertical velocity variations that are revealed by 3-D models. One of the most prominent upper mantle low velocity regions is located in the Middle East, extending from Turkey to Iran and western Afghanistan. This low velocity anomaly coincides with the Turkish-Iranian continental plateau, formed by the collision between the Arabian and Iranian Plateau. This collision is the result of the closing of the Neo-Tethys Ocean by northward subduction of oceanic lithosphere beneath Eurasia. In Iran and western Afghanistan, the low velocity anomaly is bounded to the south by high velocities, part of the Arabian plate. This low velocity anomaly is prominent in other Pn tomography studies (e.g., Hearn and Ni, 1994), and is also coincident with a region of high S-wave attenuation (Kadinsky-Cade et al., 1981) and Neogene volcanism (Kazmin et al., 1986). The combination of these observations suggests a hot or perhaps partially molten uppermost mantle beneath the Turkish-Iranian Plateau. This anomalously hot upper mantle could be a remnant of the backarc extensional regime that dominated this region from the Jurassic to the Neogene (Dercourt et al., 1986). The presence of hot, molten upper mantle weakens the lithosphere, allowing larger deformation associated with the Arabian Plate-Eurasia collision. This results in the observed diffuse intraplate seismicity that extends well to the north of the plate boundary delineated by the Zagros Main Thrust. Furthermore, the buoyancy associated with hot upper mantle, combined with the buoyancy due to the deep continental roots in the region, can contribute to maintain the high topography of the plateau.

The method for producing P_n and S_n maps with associated parametric corrections effectively summarizes the information in our large relocated catalogue data base for epicentral distances from about 3^o to 15^o. The P_n and S_n maps correlate well with other high resolution information about structural variations in the uppermost mantle. The travel time correction surfaces computed from the CU P_n/S_n model appear to be robust and fit the data with low levels of bias at epicentral distances from 3^o to 15^o. Overall rms misfits across Eurasia for P_n are ~1.5 s and for S_n~3.0 s, are better for data subsets chosen for their quality (e.g., explosions, large magnitude events, independent information about epicenter location and/or origin time), and exhibit a strong, nearly linear distance trend. These misfits are considerably better than those produced by ak135 and CRUST5.1, although ak135 fits the P data remarkably well for a 1-D model. The correction surfaces presented here provide a reference for 3-D models to match and extend. Although the method described here appears to produce reliable travel time correction surfaces, there are greater problems in estimating P_n and S_n reliably due to trade-offs between the estimated tomographic map and the parametric corrections. Some of these trade-offs can be ameliorated in the future if a 3-D model is used as the reference model, which will allow the horizontal ray approximation to be broken. Indeed, it is likely that our P_n model fits the data only marginally better than the 1-D model ak135 because a single distance correction is inadequate to model ray penetration into the upper mantle, which can be highly variable, as figure 4b indicates. Getting the vertical velocity derivative right may be more important in predicting regional travel times than mapping lateral variations. Recent models, such as those of Ekstrom and Dziewonski (1998), Villasenor et al. (2001), and Shapiro et al. (2000), are providing new information about the vertical velocity gradient in the uppermost mantle which controls the depth of penetration and, hence, a large fraction of the travel time of regionally propagating phases. In addition, to extend travel time correction surfaces beyond 15^o will require a 3-D model to predict the ray paths.

At the end we present a table (table 2) which indicates P_n and S_n velocities at 6 different regions of Iran, North Western, Central Alborz, North Eastern, Central, Eastern and South Eastern.

Table 1. Summary of misfits to the whole Iranian plate data set.

	P_n		S_n	
model	*mean (s)*	σ *(s)*	*mean (s)*	σ *(s)*
CU P_n/S_n	0.01	1.53	0.03	3.10
ak135	-0.01	1.86	-2.20	4.27
CRUST5.1	2.50	2.12	4.24	4.23

Table 2. P_n and S_n velocities in 6 different regions of Iran.

S_n (Km/s)	**P_n (Km/s)**	**Latitude**	**Longitude**	**Region**
4.4055	7.8058	35-40	45-50	1-NW Iran
4.4971	7.9233	35-40	50-55	2-Alborz
4.4961	7.9488	35-40	55-60	3-NE Iran
4.4544	7.8721	30-35	50-55	4-Central Iran
4.4378	7.8533	30-35	55-60	5-East Centarl
4.4851	7.8849	25-30	55-60	6- SE Iran

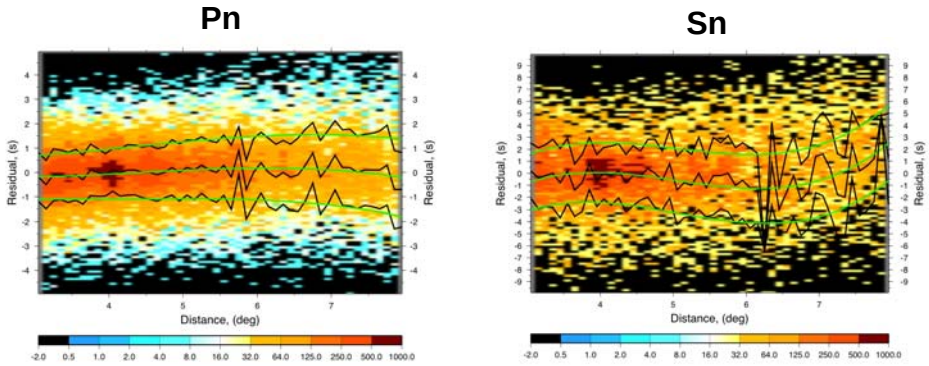

Figure 9. P_n and S_n Residuals based on Distance for CU P_n/S_n, ak135 and CRUST5.1.

ACKNOWLEDGEMENTS AND APPRECIATION

I would like to thank Mike Ritzwoller for providing me with references and resources to do this job better and more efficiently. I would like to thank Misha Barmin for letting me use his source codes to edit and rewrite my own codes for this project and finally I would like to thank Bob Engdahl for consultation on my data set.

REFERENCES

Barmin, M. P., Ritzwoller, M. H., and Levshin, A. L., 2001, A fast and reliable method for surface wave tomography, Pure Appl. Geophys., **158**, 1351-1375.

Bijwaard, H., Spakman, W., and Engdahl, E. R., 1998, Closing the gap between regional and global travel time tomography. J. Geophys. Res., **13**, 30055-30078.

Cerveny, V., and Psencik, I., 1988, Numerical modeling of seismic wave-elds in 2-D laterally varying layered structures by the ray method, in Seismological Algorithms, Academic Press, London.

Cunningham, W. D., 1988, Lithospheric controls on late Cenozoic construction of the Mongolian Altai, Tectonics, **17**, 891-902.

Dercourt, J., and 18 co-authors, 1986, Geological evolution of the Tethys belt from the Atlantic to the Pamirs since the Lias, Tectonophys., **123**, 241-315.

Ekstrom, G., and Dziewonski, A. M., 1998, The unique anisotropy of the Paci_c upper mantle, Nature, **394**, 168-172.

Engdahl, E. R., and Ritzwoller, M. H., 2001, Crust and upper mantle P- and S-wave delay times at Iranian Plateau seismic stations, Phys. Earth. Planet. In., **123**, 205-219.

Engdahl, E. R., R. van der Hilst, and Buland, R., 1998, Global teleseismic earthquake relocation with improved travel time and procedures for depth determination, Bull. Seismol. Soc. Am., **88**, 722-743.

Hearn, T., Beghoul, N., and Barazangi, M., 1991, Tomography of the Western United States from regional arrival times, J. Geophys. Res., **96**, 16369-16381.

Hearn, T.M. and Clayton, R.W., 1986, Lateral velocity variations in Southern California. I. Results for the upper crust from Pg waves, Bull. Seismol. Soc. Am., 76, 495-509.

Hearn, T. M., and James, F. N., 1994, P_n velocities beneath continental collision zones: the Turkish-Iranian plateaux, Geophys. J. In., **117**, 273-283.

Hearn, T. M., and Ni, J. F., 1994, P_n velocities beneath continental collision zonens the Turkish-Iran Plateau, Geophys. J. In., **117**, 273-283.

Kadinsky-Cade, K., Barazangi, M., Oliver, J., and Isacks, B., 1981, Lateral variations of high-frequency seismic wave propagation at regional distances across the Turkish and Iranian Plateau, J. Geophys. Res., **86**, 9377-9396.

Kazmin, V. G., Sbortshikov, I. M., Ricou, L. E., Zonenshain, L. P., Boulin, J., and Knipper, A. L., 1986, Volcanic belts as markers of the Mesozoic-Cenozoic active margin of Eurasia, Tectonophys, **123**, 123-152.

Kennett, B. L. N., Engdahl, E. R., and Buland, R., 1995, Constraints on seismic velocities in the Earth from travel times, Geophys. J. In., **122**, 108-124.

Molnar, P., 1988, A review of geophysical constraints on the deep structure of the Tibetan plateau, the Himalaya and the Karakoram, and their tectonic implications, Phil. T. Roy. Soc., **A326**, 33-88.

Molnar, P., England, P., and Martinod, J., 1993, Mantle dynamics, uplift of the Tibetan Plateau, and the Indian monsoon, Rev. Geophys., **31**, 357-396.

Mooney, W. D., Laske, G., and Masters, G., 1998, CRUST 5.1: A global crustal model at 5 degrees by 5 degrees, J. Geophys. Res., **103**, 727-748.

Myers, S. C., and C.A. Schultz, C. A., 2000, Improving sparse network seismic location with Bayesian Kriging and teleseismically constrained calibration events, B. Seismol. Soc. Am., **90**, 199-211.

Shapiro, N. M., Ritzwoller, M. H., Villaseor, A., and Levshin, A. L., 2000, Shear velocity structure of the Eurasian Plate crust and uppermost mantle, Eos T. Am. Geophys. Un., 81 (48), F861, Nov. 28.

Sultanov, D. D., Murphy, J. R., 1999, and Kh.D. Rubinstein, A seismic source summary for Soviet peaceful nuclear explosions, B. Seismol. Soc. Am., **89**, 640-647.

Tabatabai, Sh., 2007, Relocation of earthquakes and study of crust and upper mantle structures in Iranian plateau, Ph.D Dissertation in Farsi, Institute of Geophysics, University of Tehran.

Villasenor, A., Ritzwoller, M. H., Levshin, A. L., Barmin, M. P., Engdahl, E. R., Spakman, W., and Trampert, J., 2001, Shear velocity structure of Central Eurasia from inversion of surface wave velocities, Phys. Earth Planet. In., **123**, 169-184.

Windley, B. F., and Allen, M. B., 1993, Evidence for a late Cenozoic mantle plume under central Asia, Geology, **21**, 295-298.